International Journal of Applied Mathematical Research, 4 (1) (2015) 193-204
www.sciencepubco.com/index.php/IJAMR

doi: 10.14419/ijamr.v4i1.4042
Review Paper

The comparative analysis of the two dimensional Laplace equation using the Galerkin finite element method with the exact solution for various domains with triangular elemental meshing

Sarah Balkissoon, Sreedhara Rao Gunakala, Donna Comissiong, Victor Job

The University of the West Indies, Department of Mathematics and Statistics, Faculty of Science and Technology, Trinidad and Tobago
**Corresponding author E-mail:sreedhara.rao@sta.uwi.edu*

Abstract

Laplace Equation is used in many areas of studies such as potential theory and the fundamental forces of nature, Newtonian theory of gravity and electrostatics. It is used in Probability theory and Markov Chains as well as potential flows in fluid mechanics. Laplace Equation is used in various research areas and for this reason, to determine an accurate solution to this equation is of importance. In this study, the Finite Element Method is used to approximate the solution of the 2D Laplace Equation for two regions, circular and rectangular domains. These are compared to the exact solutions of the systems subjected to various physical restrictions; boundary conditions. This was done by using a mesh generator in Matlab, Distmesh, to obtain a mesh of triangular elements and then using Matlab to plot the exact and the approximated solutions as well as to determine the errors; l_1, l_2 and l_∞ norm. For these domains, the number of elements in the mesh was incremented and it was noted there was a convergence of the approximated to the actual solution. The boundary conditions were altered to observe the changes in the regions' field variable distribution (intensity values) of the Matlab plots.

Keywords: *Finite Element Method; Laplace Equation; Triangular Elements.*

1. Introduction

1.1. Laplace Equation

The partial differential equation under analysis is the Laplace Equation. The Laplace Equation is given by:

$$\triangle u = 0 \tag{1}$$

In rectangular co-ordinates (in 2D):

$$\triangle u = a_1 \frac{\partial^2 u}{\partial x^2} + a_2 \frac{\partial^2 u}{\partial y^2} = 0 \tag{2}$$

where a_1 and a_2 are constants.

In spherical co-ordinates (in 2D):

$$\triangle u = b_1 \frac{\partial^2 u}{\partial r^2} + \frac{b_2}{r}\frac{\partial u}{\partial r} + \frac{b_3}{r^2}\frac{\partial^2 u}{\partial \Theta^2} = 0 \tag{3}$$

where b_1, b_2 and b_3 are constants.

It is a linear, scalar, elliptic and steady state equation whose solution is called a harmonic function. The non-homogenous form is called Poisson Equation and is given by: $-\triangle u = f$. The Laplace equation is used in various research areas. Researchers in Biomedical Physics and Medical Sciences have used the exact solution of Laplace Equation to evaluate data collected on the tissues; this is done to determine the tissue surface tension [1]. Harmonic functions; solutions to Laplace Equation, is used in path planning problems and robotics applications. The harmonic functions allow the environment model to be updated incrementally [2].

The Laplace equation is utilized to describe physical processes in fluid mechanics, electromagnetism, potential theory and heat condition as well as probability and number theory [3]. The field variable may represent displacement, pressure, temperature, velocity and stress. More specifically, u(x,y) can be interpreted as the displacement of a membrane (where f(x,y) in the Poisson Equation may represent an external force), u(x,y) may represent the temperature of a plate (where f(x,y) in the Poisson Equation may represent an external heat source). In fluid mechanics, u(x,y) represents a potential function whose gradient is the velocity vector for a 2 dimensional fluid flow [4]. Since this equation is related to the equilibrium of systems, various boundary conditions determine different applications of the system. For example, in thermal equilibrium modeling the Dirichlet boundary condition describes the temperature distribution of the plate, where the Neumann boundary condition (normal derivative of the solution u on the boundary) represents the heat flux into the plate through the boundary. As such, if the Neumann boundary condition is 0, there is no flux through the boundary and this physically indicates an insulated plate. In terms of fluid mechanics, where u is the velocity potential, the Neumann boundary conditions can represent solid surfaces where there is no fluid flow across these walls and the Dirichlet conditions may represent openings in the domain where there is a constant horizontal velocity [4][5].

1.2. Finite Element Method (FEM)

There are various numerical methods for approximating partial differential equations. One of them is finite element method, as shown in the subsequent diagram, Fig.1. The Finite Element Method has four steps [6][7]. These are:

1. Division of the domain into a finite number of elements (e) (triangular, quadrilateral or both). The union of these elements is an estimate of the region (Ω).

2. Determination of the equations for each of the elements. In this paper, each element coefficient matrix is determined.

3. Attainment of the system's global stiffness matrix by assembling all of the elements which comprises of the domain.

4. Solving the system of equations.

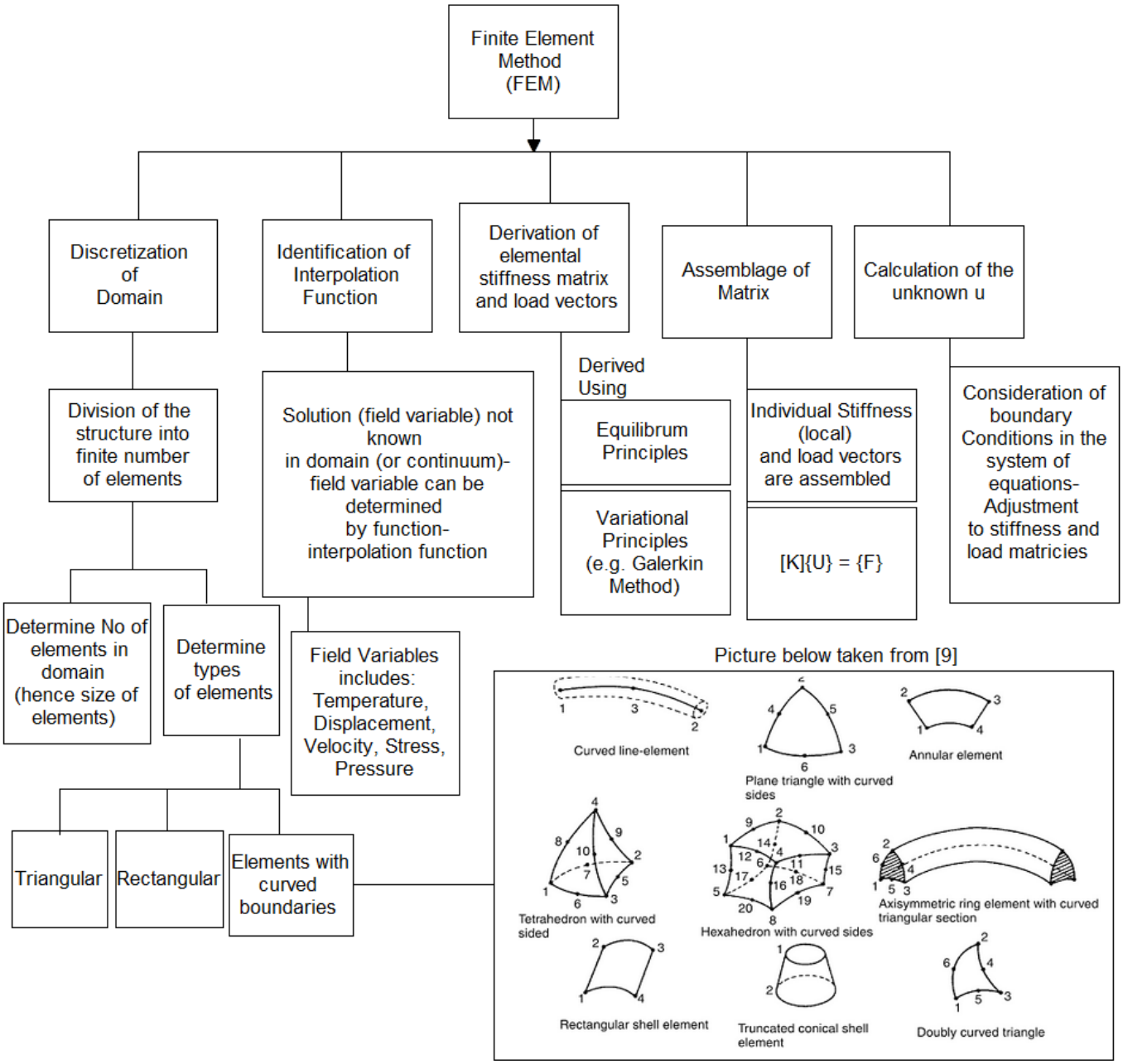

Fig.1: Flow chart illustrating the finite element method

2. Formulation of problem

This study considered circular and rectangular domains. For the rectangular domain, (2) was used when a_1 and a_2 were all 1. The governing equation for the circular region is (3). The constants b_1, b_2 and b_3 were assigned a value of 1. Subsequent figures, Fig.2 and Fig.3, show the boundary conditions for both of these domains. In this study, for the rectangular domain, each surface can either have a Neumann or a Dirichlet boundary condition; these boundary values are the constant values of c_1 to c_8 shown in Fig.2. Also, in this paper, for the circular region, the assigned boundary condition is Dirichlet; see Fig.3.

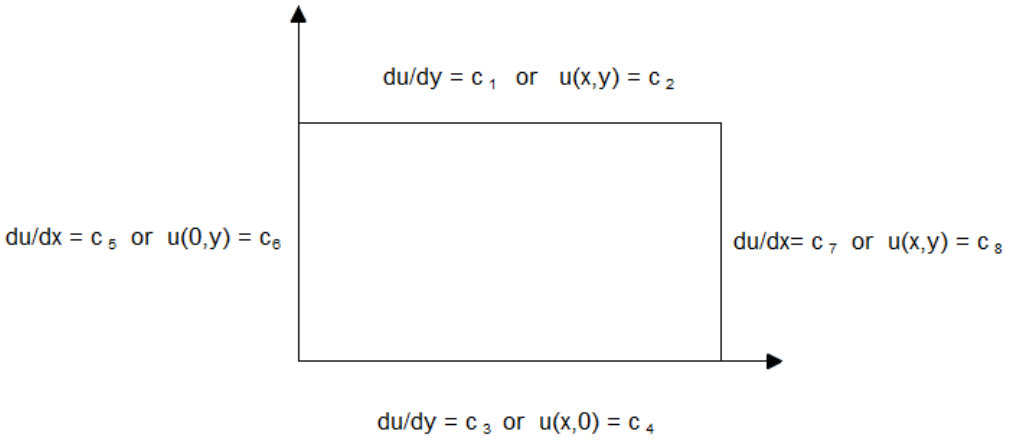

Fig.2: Rectangular domain and associated boundary conditions

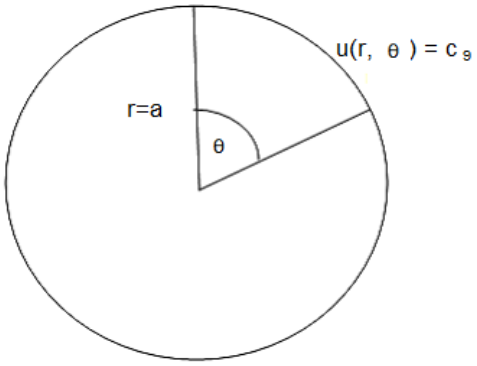

Fig.3: Circular domain and associated boundary conditions

3. FEM: Elemental equations

3.1. The weak/ residual form

The weak form is used in the finite element method because, unlike the strong form, it does not require the field variable to have strong continuity [8]. The formulations of the weak form gives rise to a system of equations when the domain is discretized. These equations give an accurate approximate solution for various domains [8]. The weak form is created in this paper using the weighted residual method.

To obtain the weak form in 2D let us consider (4) (Laplace Equation); this is given from (2) where $a_1 = a_2 = 1$.

$$\frac{\partial^2 u}{\partial x^2} + \frac{\partial^2 u}{\partial y^2} = 0. \tag{4}$$

Let w be the weight function. After multiplying by the weight function and integrating, the weighted residual integral statement, (5), was obtained.

$$\int_\Omega w \left[\frac{\partial}{\partial x}\left(\frac{\partial u}{\partial x}\right) + \frac{\partial}{\partial y}\left(\frac{\partial u}{\partial y}\right)\right] d\Omega = 0 \tag{5}$$

where Ω is the 2D domain; $(x, y) \in \Omega$.

The second order derivatives was reduced to first order using (6) and (7).

$$\int_{\Omega} w\frac{\partial F}{\partial x}d\Omega = -\int_{\Omega} F\frac{\partial \Omega}{\partial x}d\Omega + \oint_{\Gamma} wFn_x d\Gamma, \tag{6}$$

$$\int_{\Omega} w\frac{\partial F}{\partial y}d\Omega = -\int_{\Omega} F\frac{\partial \Omega}{\partial y}d\Omega + \oint_{\Gamma} wFn_y d\Gamma, \tag{7}$$

where Γ is the boundary of the 2D domain.

The elemental weak form is given by (9).

$$-\int_{\Omega} \frac{\partial u}{\partial x}\frac{\partial w}{\partial x}d\Omega + \oint_{\Gamma} w\frac{\partial u}{\partial x}n_x d\Gamma - \int_{\Omega} \frac{\partial u}{\partial y}\frac{\partial w}{\partial y}d\Omega + \oint_{\Gamma} w\frac{\partial u}{\partial y}n_y d\Gamma = 0, \tag{8}$$

$$\int_{\Omega} \left[\frac{\partial u}{\partial x}\frac{\partial w}{\partial x} + \frac{\partial u}{\partial y}\frac{\partial w}{\partial y}\right] d\Omega = \oint_{\Gamma} w\left[\frac{\partial u}{\partial x}n_x + \frac{\partial u}{\partial y}n_y\right] d\Gamma. \tag{9}$$

According to [9], (10) is the approximate solution over an element.

$$u^e = \sum_{j=1}^{n} u_j^e \varphi_j^e(x, y). \tag{10}$$

Using (9) and (10), we get (11); the i^{th} equation of element e

$$\int_{\Omega} \left[\frac{\partial}{\partial x}\left(\sum_{j=1}^{n} u_j^e\varphi_j^e\right)\frac{\partial \varphi_i^e}{\partial x} + \frac{\partial}{\partial y}\left(\sum_{j=1}^{n} u_j^e\varphi_j^e\right)\frac{\partial \varphi_i^e}{\partial y}\right] d\Omega = \oint_{\Gamma} \varphi_i^e\left[\frac{\partial}{\partial x}\left(\sum_{j=1}^{n} u_j^e\varphi_j^e\right)n_x + \frac{\partial}{\partial y}\left(\sum_{j=1}^{n} u_j^e\varphi_j^e\right)n_y d\Gamma\right]. \tag{11}$$

The global elemental force vector, elemental vector and global stiffness matrix are given by (12), (13) and (14) respectively.

$$F_i^e = 0, \tag{12}$$

$$Q_i^e = \oint_{\Gamma} \varphi_i^e q_n d\Gamma, \tag{13}$$

$$K_{ij}^e = \int_{\Omega} \left(\frac{\partial \varphi_j^e}{\partial x}\frac{\partial \varphi_i^e}{\partial x} + \frac{\partial \varphi_j^e}{\partial y}\frac{\partial \varphi_i^e}{\partial y}\right) d\Omega. \tag{14}$$

3.2. Elements in the mesh

The domain is discretized into a meshing of triangular elements. These actual elements are converted to the master element for the sake of computational purposes. Fig.4 illustrates this below.

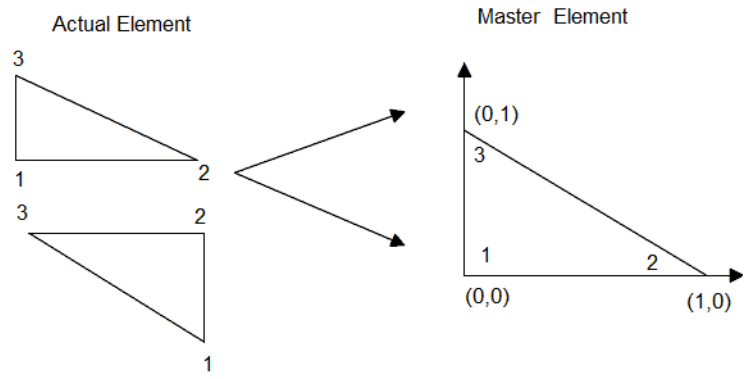

Fig.4: Conversion of actual to master element

The approximate solution, u, is represented as a linear combination of undetermined coefficients and approximating functions called interpolation functions [9]; refer to (10). The shape functions used for co-ordinate interpolation are written in terms of the master elements co-ordinates, (ξ, η) as seen in (15), (16) and (17). These shape function are:

$$\psi_1 = 1 - \xi - \eta, \tag{15}$$

$$\psi_2 = \xi, \tag{16}$$

$$\psi_3 = \eta. \tag{17}$$

The elemental Jacobian transformation matrix given in (18) was used to convert from actual to master element.

$$\left[J^e\right] = \begin{bmatrix} \frac{\partial \psi_1}{\partial \xi} & \frac{\partial \psi_2}{\partial \xi} & \frac{\partial \psi_3}{\partial \xi} \\ \frac{\partial \psi_1}{\partial \eta} & \frac{\partial \psi_2}{\partial \eta} & \frac{\partial \psi_3}{\partial \eta} \end{bmatrix} \begin{bmatrix} x_1^e & y_1^e \\ x_2^e & y_2^e \\ x_3^e & y_3^e \end{bmatrix}. \tag{18}$$

4. Finite element approximation: results and discussion

Distmesh [10] was used in Matlab to generate a mesh as well as the boundary nodal points. The mesh generated was then used in this numerical approximation method to determine an approximation of u. The finite element solution has three sources of error. These are the errors which are obtained from approximating the domain as well as the solution and the numerical computational errors, which can be derived from round off errors from the computer [9]. The determination of these errors is difficult, but can be estimated for a particular element and problem [9]. However in this study, the difference between the approximate U (the finite element solution) and the known solution u (exact/known solution of the Laplace), U-u is computed. This difference determines the accuracy of the finite element solution. The accuracy of the approximation according to [9] is established from, the differential equation, the integral form as well as the types of elements used in the meshing. In this paper, the relative norm error was determined, that is the ratio of the error between FEM approximation and exact solution. The convergence property of the finite element solution to the exact solution was also investigated by increasing the number of nodes.

4.1. Circular domain

The Laplace Equation, $\Delta u = 0$, satisfies the Dirichlet boundary condition on the unit circle. A circular disc of radius 1 is considered. We have the Dirichlet boundary value problem with $u(1, \Theta) = \Theta$ for $-\pi \leq \Theta \leq \pi$. Thus from figure 3, we take $r = 1$ and $c_9 = \Theta$. This boundary condition is indicative of a "wire in a single turn of a

spiral helix sitting over a unit circle". There is a jump discontinuity of magnitude 2π at the point (-1,0) [4]. The solution of this problem is given by (19).

$$u(r,\Theta) = 2\left(rsin\Theta - \frac{r^2 sin2\Theta}{2} + \frac{r^3 sin3\Theta}{3} - \frac{r^4 sin4\Theta}{4} + ...\right). \tag{19}$$

Matlab plots were generated for the exact solution and the FEM approximated solution for this system. The graphical results shows similarities between the approximate and exact solution. We can see that the field variable has a greater value (indicative of the red region) in the upper part of the disc and from the colour scale, is quantitatively less in the lower region. There is no external heat source present as it is not a Poisson Equation. Also from the given boundary conditions, there is no specified concentration gradient and no diffusion taking place since these conditions are not Neumann. If the field variable is temperature, this problem can arise from a plate with a high temperature on the upper region of the disc. The temperature distribution of the plate (described by the Dirichlet boundary condition) for the approximate FEM solution increases in accuracy (when compared to the actual solution) as the number of nodes is increased. Fig.5 and Fig.6 show the graphical results from the numerical simulation.

Number of Elements = 1045

Exact Solution Approximate Solution

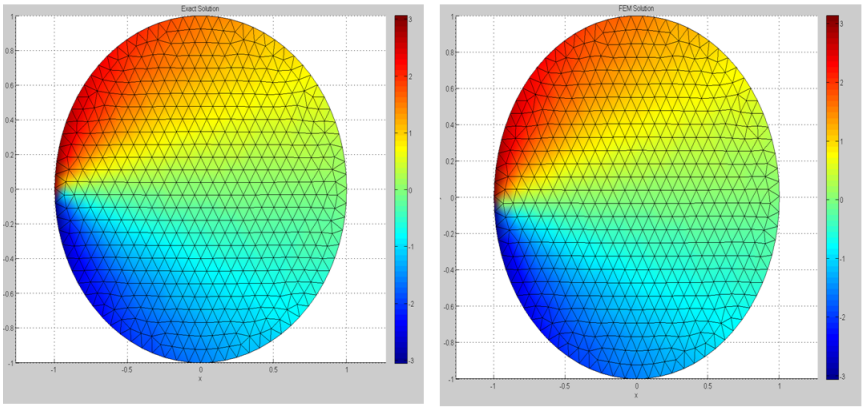

Fig.5: Approximate solution and FEM solution of system consisting of 1045 elements

Number of Elements = 2774

Exact Solution Approximate Solution

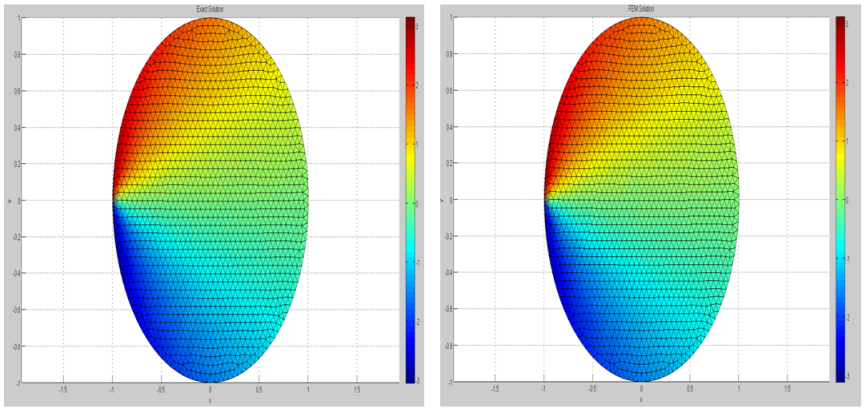

Fig.6: Approximate solution and FEM solution of system consisting of 2774 elements

Table 1: Errors of the approximated solution for varying number of elements in the circular domain

Number of Elements	l_1 norm	l_2 norm	l_∞ norm
1045	0.0336	0.0647	0.3378
1385	0.0140	0.0267	0.1500
1910	0.0060	0.0115	0.0756
2774	9.4896×10^{-4}	0.0030	0.0217

The above table shows convergence of the approximated finite element solution to the exact solution when the number of elements was incremented.

The analysis done in this paper are with three norms l_1, l_2 and l_∞. These norms represent the distance or size of a vector or matrix [11]. These norms were calculated for the difference between two vectors, the approximate and the exact solutions. The l_1, l_2 and l_∞ norms and their vector differences are given by (20) to (21), (22) to (23) and (24) respectively [11]. In this study, for these norms, the relative difference between these two vectors were calculated.

l_1 norm:

$$\|U\|_1 = \sum_i |U_i| \,. \tag{20}$$

Sum of absolute difference:

$$\|U - u\|_1 = \sum_i |U_i - u_i| \,. \tag{21}$$

l_2 norm:

$$\|U\|_2 = \sqrt{\sum_i U_i^2}. \tag{22}$$

Euclidean distance:

$$\|U - u\|_2 = \sqrt{\sum_i (U_i - u_i)^2}. \tag{23}$$

l_∞ norm:

$$\|U\|_\infty = max(|U_i|). \tag{24}$$

Table 1 shows that the l_∞ norm has the greatest error values when compared to the other two norms. This is consistent with the theory because from (24), it is given that this norm gives the maximum error. The l_1 norm values are approximately half the size of the l_2 norm values and the l_∞ norm is roughly ten times its value. However, all of these three norms indicated convergence of the approximate solution U to the actual solution u of the system. This is so because as the number of elements of the domain increased, the numerical values of the various norms tended to 0.

From Fig.3, c_9 was then changed to $sin\Theta$ and then to $cos\Theta$. The Dirichlet boundary conditions were $u(1, \Theta) = sin\Theta$ and $u(1, \Theta) = cos\Theta$ respectively (both are 2π periodic). From the results obtained in Fig.7, it is noted that there is a pattern from region of most intensity value to the region of least intensity value from the field variable distribution maps. This could have been as a result of the periodicity of Dirichlet boundary conditions. When the boundary condition used was sinΘ, we see that the field variable is greatest in the region to the left of the disc whilst it is on the right for the imposed boundary condition of cosΘ. This could be as a result of the phase difference between these two periodic waves.

Approximate Solution

B.C: $u(1,\Theta) = sin\Theta$

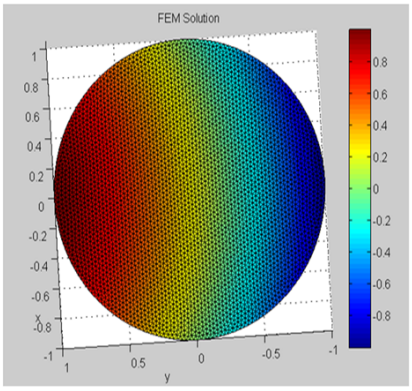

Approximate Solution

B.C: $u(1,\Theta) = cos\Theta$

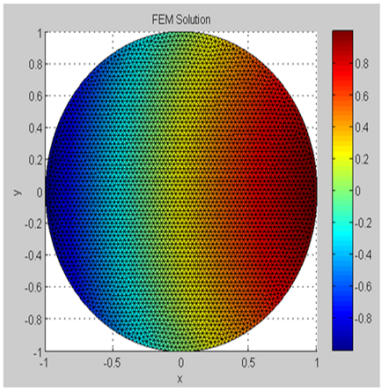

Fig.7: FEM approximated solution plot for varying boundaries

4.2. Rectangular domain

From Fig.2, only Dirichlet boundary conditions are imposed on the system. The boundary values of these Dirichlet conditions are $c_2 = c_4 = c_8 = 0$ and $c_6 = 1$. In thermal equilibrum modeling, these applied boundary conditions indicate that all of the surfaces except u(x,0) have a fixed temperature of 0. There is no specified normal derivative of the field variable, temperature, at each point of the boundary. This is representative of Neumann boundary conditions. There are no external heat sources as there is no f(x,y) term. In fluid mechanics, from these boundary conditions, the potential function is non-zero when $y = 0$.

We now repeat this with a rectangular domain, Matlab plots were generated; these can be seen in both Fig.8 and Fig.9. The graphical results for varing number of triangular meshed elements; for both the actual and approximated solutions, were compared. From the figures below, we see that all the boundaries except the surface of u(x,0) have the least value, 0, as indicated from the dark blue scaling in the map legend. The surface of u(x,0) however, has the highest colour scaling of red which has a numeric value of 1 in the map legend. This is indicative of the imposed boundary conditions of the system. This can be a physical representation of having this fixed non-zero temperature at the boundary u(x,0) and maintaining the other boundary values at 0. This is a system with steady state temperature distribution. When comparing Fig.8 with Fig.9, it is evident that as the domain is divided into more elements, the temperature distribution becomes more accurate.

Number of Elements = 614

Exact Solution

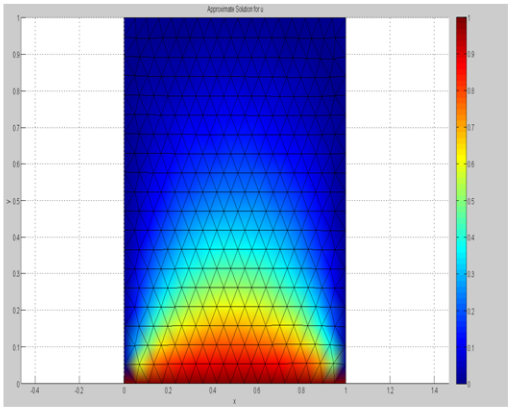

Approximate Solution

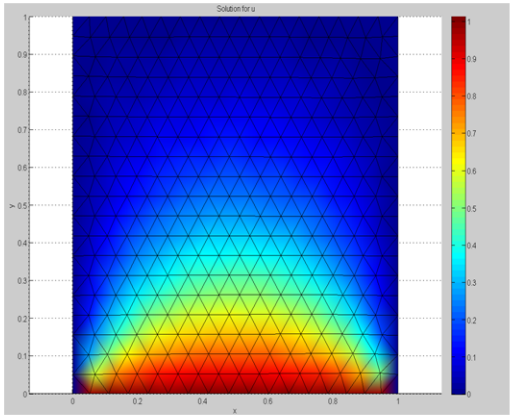

Fig.8: Approximate solution and FEM solution of system consisting of 614 elements

Number of Elements =2476

Exact Solution Approximate Solution

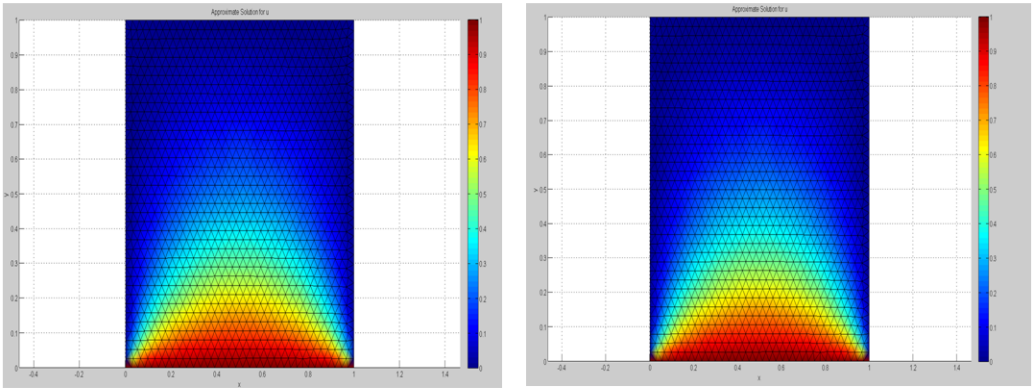

Fig.9: Approximate solution and FEM solution of system consisting of 2476 elements

This is also noted from the numerical error analysis shown in Table 2. As the number of elements was increased to give a range of 256-2476 elements, the accuracy of the finite element approximated solution increases and convergence to the exact solution was noted. The l_1 norm which gives the least error, decreased from 0.0574 to 0.0075 when 2220 triangular elements were added to the mesh (0.0499 decrease in the error value).

Table 2: Errors of the approximated solution for varying number of elements in the rectangular domain

Number of Elements	l_1 norm
256	0.0574
899	0.0186
1374	0.0123
2476	0.0075

The mathematical model was changed to a system of two Dirichlet and two Neumann bounary conditions. The Neumann boundary values were $c_1 = c_3 = 0$ and the Dirichlet bounday values, c_6 and c_8 were 300 and 400 respectively. As anyalzed previously, the Dirichlet conditions can represent the temperature distribution of the domain. Since there are two Neumann boundary conditions and these are 0 in value, the flux through the boundary is 0. Thus these two boundaries represent insulated surfaces.

This above-mentioned mathematical formulation is important in the study of advanced works in electromagnetism [12][13]. However most of the studies being done with Laplace equation considers Dirichlet Boundary Conditions because there are not many physical applications for a formulation with both Dirichlet and Neumann boundary conditions. One experimental application is a two dimensional electrostatic problem. The experimental procedure consisted of a dipolar configuration where 2 electrodes are placed in the domain which contains liquid with electrical conductivity. This will be the study of field lines and equipotential surfaces. An alternating current is used in the experiment of a specified frequency. This ensures that there is a constant potential distribution. Since the range of the frequency used yields a much higher electromagnetic field wavelength than that of the experiment, the electric field is quasistatic. Thus this can be considered as a electrostatic case (the charges are almost stationary with no acceleration). The electrostatic distribution is the same as the potential distribution [13].

The non-conducting wall (horizontal surface) of the rectangular container satisfies the Neumann boundary condition and the conducting wall satisfies the Dirichlet boundary condition (horizontal surface). The current density in liquid flows parallel to the walls of the non-conducting container, hence there is no perpendicular flow of current density to these walls. This gives $\frac{\partial V}{\partial n} = 0$, the Neumann boundary condition. Here $u = V$ is the potential and $y = n$ is the direction perpendicular to the surface. The Dirichlet boundary conditions are given by having two conducting walls [13].

When the field variable is velocity potential, the Dirichlet boundary conditions represent openings and the Neumann conditions represent solid surfaces of rectangular region [5]. In this domain, the velocity is horizontal and of constant value 300 and 400, and there is no velocity normal to the solid walls. This is a restiction of vertical flow (see Fig.10). On the boundary u(0,y), we see a colour scale of blue with 300 in the legend. At the parallel boundary we obtain the largest value of the scale which is 400. On the two horizontal boundaries with Neumann boundary conditions, it is noted that the colour scale spans from 300 to 400; taking its least and greatest velocities at the corners of the domain. It takes the value of 300 at the corners of the horizontal walls with the Dirichlet boundary of u(0,y), and 400 at the corners of these walls and the wall of u(a,y).

This Matlab generated plot for the approximate solution of u can be seen below.

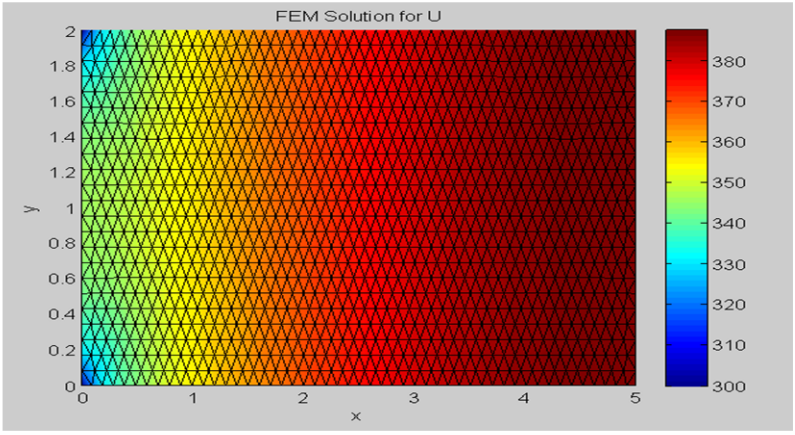

Fig.10: Approximate FEM solution

5. Conclusion

There were three parameters taken into consideration; the number of nodes, the types of domains and the boundary conditions imposed on the system. From the results, we determined that when the domain had an increased number of meshed triangular elements, the accuracy of the finite element approximate solution increased. We can see this from the reduction of the l_1, l_2 and l_∞ norms as the number of elements was increased. Evidence of this was given via graphical Matlab plots as well. The next investigation was to determine how the solution changes with the boundary conditions. The plots were analyzed to determine the variations in the field values when restrictions were placed on the domains. As expected, when various boundary conditions were applied, there were variations in the colour map. This is a useful tool, as various systems can be modeled under different boundary conditions which can be interpreted as a mathematical representation of a physical restriction of the system. The third variable was the changing of the domains. The Laplace Equation was subjected to two different domains; rectangular and circular (hence a change in co-ordinate systems from rectangular to polar). We can conclude that the FEM is an effective and accurate procedure to determine the approximate solution of a system subjected to various physical constraints, regardless of the domains of this study.

References

[1] C. Norotte et al., Experimental evaluation of apparant tissue surface tension based on the exact solution of the Laplace Equation, *A letters Journal Exploring the Frontiers of Physics*, (2008).

[2] C.I. Connolly and R.A Grupen, On the Applications of harmonic functions to robotics,*Journals of Robotic Systems*, (1993), pp.931-946.

[3] S.S. Rao, Finite Element Method in Engineering, Fourth Edition,*Elsevier Science and Technology Books*, (2004).

[4] P.J. Olver, Introduction to Partial Differential Equations, *Springer*, (2014).

[5] G.E. Urroz, Utah State University Department of Civil and Environmental Engineering. Solutions to a potential flow in a rectangular domain. http://ocw.usu.edu/Civiland Environmental Engineering/Numerical Methods in Civil Engineering/PotentialFlowRectangularDomain.pdf. Revised October 2004. Accessed April 15, (2014).

[6] P.V. Patil and J.S.V.R.K. Prasad, Solution of Laplace Equation using Finite Element Method, *Pratibha: International Jounal of Science, Spirituality, Business and Technology*, Vol.2, (2013),pp.40-46.

[7] P.V. Patil and J.S.V.R.K. Prasad, Numerical solution for two dimensional Laplace Equation with Dirichlet boundary conditions, *IOSR Journal of Mathematics*, Vol.6, (2013), pp.66-75.

[8] G.R. Liu and S.S Quek, The Finite Element Method A practical course, *Elsevier Science Ltd*, (2003).

[9] J.N. Reddy, An Introduction to the Finite Element Method, Third Edition, *McGraw-Hill, New York City*, (2006).

[10] P-O. Persson and G. Strang, A simple mesh generator in MATLAB, *SIAM Review*, Vol.46, No.2, (2004), pp.329-345.

[11] E. Isaacson and H.B. Keller, Analysis of Numerical Methods, *Courier Dover Publications*, (1994).

[12] M. Shabbir, M. Rafiq, M.O. Ahmed, A. Pervaiz and R. Siddique, Finite Element solution for two dimensional Laplace Equation with Dirichlet boundary conditions, *Pak. J. Engg. and Appl. Sci*, Vol.10, (2012), pp.97-102.

[13] S. Gil, M.E. Saleta and D. Tobia, Experimental study of the Neumann and Dirichlet boundary conditions in two-dimensional electrostatic problems, *American Journal of Physics*, Vol.70, No.12, (2002), pp.1208-1213.